Original Article

Effects of region of interest sizes on apparent diffusion coefficient measurements of pleomorphic adenoma, Warthin tumor, and normal parotid parenchyma

Qi Sun[1#], Chao Ma[2#], Minjun Dong[1], Mengda Jiang[1], Xiaofeng Tao[1]

[1]Department of Radiology, Shanghai Ninth People's Hospital, Shanghai Jiao Tong University School of Medicine, Shanghai 200011, China; [2]Department of Radiology, Changhai Hospital of Shanghai, The Naval Military Medical University, Shanghai 200433, China

[#]These authors contributed equally to this work.

Correspondence to: Minjun Dong, MD; Xiaofeng Tao, MD. Department of Radiology, Shanghai Ninth People's Hospital, Shanghai Jiao Tong University School of Medicine, No. 639 Zhizaoju Road, Shanghai 200011, China. Email: peter_dongmj@yeah.net; cjr.taoxiaofeng@vip.163.com.

Background: Tumor apparent diffusion coefficient (ADC) measurements may be influenced by region of interest (ROI) sizes; however, this effect has not been systematically studied in parotid tumors. Our purpose was to determine the effects of ROI size on ADC measurements for the differentiation of pleomorphic adenoma (PA), Warthin tumor (WT), and normal parotid parenchyma.

Methods: Sixty-five patients including 37 with PA (lesions, n=37) and 28 with WT (lesions, n=36) were examined with diffusion-weighted imaging (DWI). Participants with normal contralateral parenchyma of the parotid gland constituted the control group (n=56). The mean ADC values and standard deviations (SDs) of the ADC (ADC_{SD}) of 12 concentric round ROIs (areas: 9, 28, 34, 50, 60, 82, 93, 98, 115, 130, 136, and 149 mm^2) for tumors and normal tissue were measured by using custom-made software. Homogeneity index, which was defined by the ADC_{SD}/mean ADC, was also calculated. One-way repeated analyses of variance (ANOVAs) were performed on the mean ADCs, ADC_{SD}s, and homogeneity indices of the 12 ROIs in each group. The three parameters at different ROIs among PA, WT, and normal parotid parenchyma were compared using Kruskal-Wallis tests.

Results: There was excellent agreement for the ADC measurements with the 12 ROIs for PA [intraclass correlation coefficient (ICC), 0.98], WT (ICC, 0.99), and normal parotid parenchyma (ICC, 0.95). No significant differences were observed in the mean ADCs of the 12 ROIs for each of the three groups (P=0.744–0.990). Among the three groups, the mean ADC of normal parotid parenchyma [$(0.94\pm0.003)\times10^{-3}$ mm^2/s] was significantly lower than that of both PA [$(1.72\pm0.01)\times10^{-3}$ mm^2/s] and WT [$(1.16\pm0.01)\times10^{-3}$ mm^2/s] in the 12 ROIs, whereas the PA group had the highest mean ADC values. No significant differences were found in the mean ADC_{SD}s with each ROI between PA and WT (all P>0.017). PAs had lower homogeneity indices compared with WTs and normal parotid parenchyma (all P<0.01).

Conclusions: The effect of ROI size on ADC measurements could be excluded from the differentiation of PA, WT, and normal parotid parenchyma. Homogeneity index was a useful parameter in discriminating between the three groups.

Keywords: Diffusion-weighted imaging (DWI); apparent diffusion coefficient (ADC); region of interest (ROI); pleomorphic adenoma (PA); Warthin tumor (WT)

Submitted Jun 11, 2018. Accepted for publication Apr 17, 2019.
doi: 10.21037/qims.2019.04.11
View this article at: http://dx.doi.org/10.21037/qims.2019.04.11

Introduction

Magnetic resonance imaging (MRI) has become increasingly important in the diagnosis and evaluation of various diseases in clinical practice because of the advantages of multiple soft-tissue contrasts and absence of ionizing radiation. For parotid gland tumors, MRI is valuable for identifying tumor location and extension, and the relationship between the tumor and the facial nerve (1-14). As a functional method of MRI, diffusion-weighted imaging (DWI) with derived apparent diffusion coefficient (ADC) can provide useful information in the differentiation of various entities of parotid tumors (15). Yerli *et al.* reported that MRI combined with DWI seemed to have similar diagnostic potential as fine-needle biopsy in the differentiation of benign and malignant parotid masses (4).

Some studies have investigated the possibility of predicting different parotid gland tumors by using DWI with ADC (16,17). However, the reported range of ADCs for parotid masses varies dramatically across different studies [e.g., pleomorphic adenoma (PA): 1.442×10^{-3} to 2.09×10^{-3} mm^2/s; Warthin tumor (WT): 0.756×10^{-3} to 1.85×10^{-3} mm^2/s; malignant tumor: 1.05×10^{-3} to 1.51×10^{-3} mm^2/s] (2-6,10,18-20), which may be caused by variation in sizes of the region of interest (ROI) (21–1,474 mm^2) (2,3,10,17). Many contradictions and arguments inevitably arise between studies, and these issues remain unresolved. Recently, some authors have reported on the influences of ROI on ADC measurements of pancreatic cancer, rectal cancer, etc. (21,22). However, the effects of ROI size on ADC measurements in PA, WT, and normal parotid parenchyma have not been systematically studied. Therefore, the purpose of our study was to assess the influence of ROI size on ADC measurements for differentiating PA, WT, and normal parotid parenchyma.

Methods

Subjects

From June 2015 to August 2017, 37 patients (male, 16; mean age, 42.8±15.4 years; range, 12–73 years) with pathologically proven PA (37 lesions) and 28 patients (male, 27; mean age, 59.1±11.1 years; range, 36–86 years) with pathologically proven WT (36 lesions) were enrolled. Nine patients had bilateral WT. The mean lesion sizes were 25.68±9.23 mm (range, 16–46 mm) and 24.93±9.05 mm (range, 15–53 mm) for PA and WT, respectively. All of the lesions were removed surgically, and final diagnosis was performed by histopathological examination of surgical specimens. The ethics committee of our hospital approved this retrospective study, and informed consent was waived for all participants.

MRI procedure

All 65 participants preoperatively underwent MRI examinations on a 3.0-T system (Ingenia, Philips Healthcare Systems, The Netherlands) with a 20-channel phased array head and neck coil. Conventional MRI protocols including transversal single-shot echo-planar DWI (b-values of 0 and 1,000 s/mm^2) were used. The main scan parameters and the scanning order of MRI sequences are presented in *Table 1*.

Data analysis

A mono-exponential fitting model [$ADC = \ln(SI_{b0}/SI_{b1000})/1{,}000$] was used for the ADC map calculation on a workstation (EWS, Extended WorkStation, Ingenia, Philips Healthcare Systems). "SI_{b0}" and "SI_{b1000}" indicate the signal intensity of the DWI on b =0 and 1,000 s/mm^2, respectively. The "ln" represents the natural logarithm. MRI data of patients were anonymous and disorganized. Custom-made software was used for the ADC measurements with defined 12 concentric round ROIs (areas: 9, 28, 34, 50, 60, 82, 93, 98, 115, 130, 136, and 149 mm^2). The largest ROI was set to 149 mm^2 considering the smallest lesion was 15 mm in the study to make the ROI locatable in the lesion. The ADCs of PA, WT, and normal parotid parenchyma measured twice by two observers by consensus (*Figure 1*). ROIs were placed on the solid part of tumors and the normal parotid parenchyma. The standard deviation (SD) of the ADC (ADC_{SD}) of each ROI was also calculated and recorded.

Statistical analysis

Medcalc software (Version 13.0.0.0, MedCalc Software, Belgium) was used for statistical analyses. The intraclass correlation coefficients (ICCs) were calculated for the two ADC measurements. The homogeneity indices (defined by the SD/mean ADC within each ROI) were calculated for the tumors/tissue at each ROI (23). The mean ADCs and ADC_{SD}s were averaged between the two measurements for further analyses. One-way repeated analysis of variance (ANOVA) was used for the comparisons of mean ADCs, ADC_{SD}s, or homogeneity indices of 12 ROIs in each group

Table 1 The main parameters of MRI protocol

Sequences	TR/TE (ms)	FOV (mm)	Matrix	Thickness/ gap (mm)	Flip angle (°)	Slices	NSA	Bandwidth (kHz)	Speed factor
T2WI	3,000/85	240×240	368×209	4/0.4	90	24	2	514.6	1.8
DWI	2,250/68	190×222	192×192	4.5/0.45	90	14	5	37.8	2.5
T1WI	600/18	240×240	300×240	4/0.4	90	24	1.5	218.2	1.2

MRI, magnetic resonance imaging; TR, repetition time; TE, echo time; FOV, field of view; NSA, number of signal averaged; T2WI, T2-weighted imaging; DWI, diffusion-weighted imaging; T1WI, T1-weighted imaging.

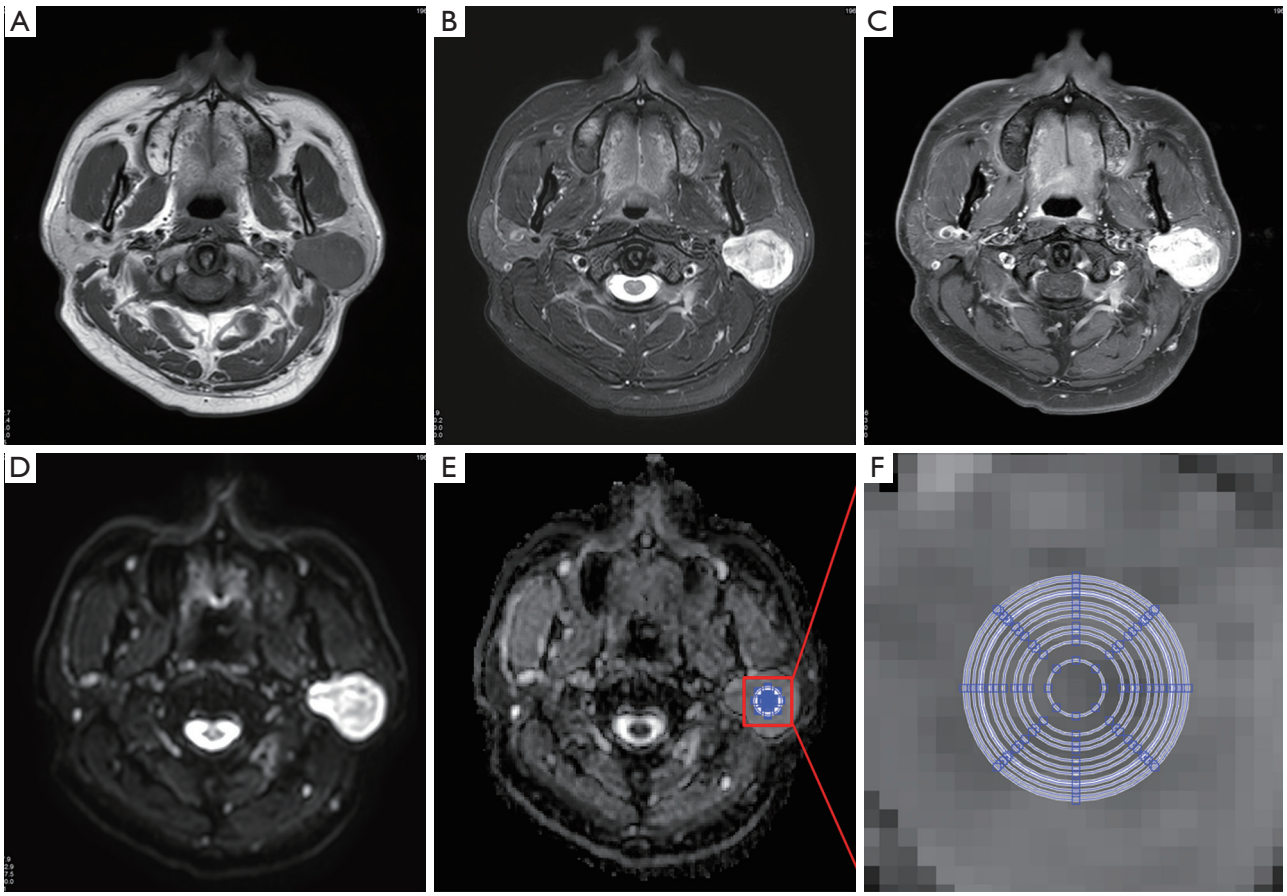

Figure 1 Apparent diffusion coefficient (ADC) measurements of Warthin tumor. (A) Axial T2WI; (B) axial pre-contrast T1-weighted image (T1WI); (C) axial contrast-enhanced T1WI; (D) diffusion weighted image (b =1,000 s/mm^2) with clearly demarcated hyperintensity compared with the surrounding and contralateral parotid gland tissues; (E) ADC map; (F) zoomed-in ADC map indicating the 12 concentric round regions of interest (areas: 9, 28, 34, 50, 60, 82, 93, 98, 115, 130, 136, and 149 mm^2) used for mean ADC measurements.

of PA, WT, and normal parotid parenchyma. Statistically difference was defined as a P value <0.05 in a two-sided test. The comparisons of mean ADCs, ADC_{SD}s, and homogeneity indices for each ROI size among the three groups were performed using Kruskal-Wallis tests and *post-hoc* analyses with Conover test. Additionally, receiver-operating characteristic (ROC) analyses were conducted to determine the diagnostic performances of the three parameters for differentiating between PA, WT, and normal parotid parenchyma.

Results

For the repeated ADC measurements, there was good or excellent agreement (ICC, 0.78–0.99) between the two measurements of PA, WT, and normal parotid parenchyma for all the 12 ROIs. For the ADC values of the 12 ROIs for PA, WT, or normal parotid parenchyma, there were excellent agreements with ICCs 0.98, 0.99 and 0.95, respectively. For mean ADC_{SD} values, good or excellent agreements (ICC, 0.63–0.97) were found for the 12 ROIs between the two measurements of PA or WT. In the normal parotid parenchyma, similar findings (ICC, 0.66–0.87) were observed except in the ROI with an area of 9 mm^2.

The mean ADCs of the PA, WT, and normal parotid parenchyma with the 12 ROIs ranged from 1.71×10^{-3} to 1.73×10^{-3} mm^2/s, from 1.15×10^{-3} to 1.17×10^{-3} mm^2/s, and from 0.94×10^{-3} to 0.95×10^{-3} mm^2/s respectively. ANOVA results revealed that there were no significant differences in mean ADCs with the 12 ROIs for all three groups (P=0.744–0.990). Significant differences were found for the mean ADCs among the three groups with each defined ROI. The *post-hoc* results showed that the mean ADCs of PA were the highest in the three groups (P<0.017). In addition, the mean ADCs of WT were higher than those of normal parotid parenchyma (P<0.017) with each defined ROI. The mean ADC_{SDS} of the PA, WT, and normal parotid parenchyma with 12 ROIs ranged from 0.09×10^{-3} to 0.21×10^{-3} mm^2/s, from 0.11×10^{-3} to 0.23×10^{-3} mm^2/s, and from 0.14×10^{-3} to 0.25×10^{-3} mm^2/s respectively. ANOVA results revealed that the differences of mean ADC_{SDS} obtained from the 12 ROIs were significant for all three groups (all P<0.001). No significant differences in the mean ADC_{SD}s with each ROI between PA and WT (all P>0.017). For the homogeneity indexes, the mean homogeneity indexes of the PA, WT, and normal parotid parenchyma with 12 ROIs ranged from 0.05 to 0.13, from 0.10 to 0.19, and from 0.16 to 0.27, respectively. ANOVA results revealed that the differences of mean homogeneity indexes obtained from the 12 ROIs were significant for all three groups (all P<0.001). Significant differences were found for the mean homogeneity indices among the three groups with each defined ROI (all P<0.001). PAs had a significantly lower homogeneity index compared with WTs and normal parotid parenchyma (all P<0.01). The parameters of the three groups with the 12 ROIs are summarized in *Table 2* and presented in *Figure 2* with box plots.

ROC analysis results revealed no differences in the accuracy of the ADCs in differentiating between any two groups of PA, WT, and normal parotid parenchyma (*Tables 3-5*) when the ROI size was ≥9 mm^2. For the homogeneity index, the values of area under curve (AUC) for differentiating PA from WT, PA or WT from normal parotid parenchyma were 0.730–0.749 (*Table 5*), 0.915–0.955 (*Table 3*), and 0.723–0.793 (*Table 4*) respectively. There were no differences in the accuracy of the homogeneity index in differentiating between PA and WT or normal parotid parenchyma for the 12 ROIs (all P>0.05). Similar findings were observed in differentiating between WT and normal parotid parenchyma when the ROI size was above 9 mm^2.

Discussion

MRI is a useful tool for discriminating between benign and malignant parotid gland tumors. As a functional MRI technique, DWI can be used to non-invasively explore the Brownian motion of water molecules *in vivo*. The quantified ADC can be used to measure the changes in composition of tissues (2-6,8,14-20,24,25). In parotid imaging, DWI is helpful for parotid tumor detection, and a few studies have reported that WT had lower ADCs than those in PA (3,4,10,13,18,25). In our study, the mean ADC of WT was also significantly lower than that of PA for the 12 ROIs, which is in agreement with previously reported results.

No formal recommendation has been reported for ADC measurements for parotid lesions, and few studies assessed the influence of ROI on ADC measurements in PA, WT, and normal parotid parenchyma. Previous studies using ROI sizes for ADC measurements of parotid tumors vary greatly, ranging from 21 to 1,474 mm^2 (2,3,10,17). Fruehwald-Pallamar *et al.* reported the difference in ADC values for PA and WT by using large ROIs and a standard-size ROI (round, 0.5 cm^2) respectively (20). However, the study did not report comparisons of the ADCs for the PA or WT groups using the two ROIs. Notably, the present results indicate that ROI has no significant influence on differentiating between PA, WT, and normal parotid parenchyma (P=0.744–0.990). The ADC_{SD}s or homogeneity index increased with increasing ROI size for PA, WT, or normal parotid parenchyma. However, ROC analysis results revealed no differences in the accuracy of the homogeneity index in differentiating between any two groups for PA, WT, and normal parotid parenchyma for the 12 ROIs (all P>0.05) when the ROI size was above 9 mm^2. We also found that the ICCs were increasing with the ROI sizes for the ADC measurements between the two measurements (despite good or excellent agreement with ICC, 0.78–0.99)

Table 2 Mean ADC values ($\times 10^{-3}$ mm^2/s), ADC_{SD}, and homogeneity indices of pleomorphic adenomas (PAs), Warthin tumors (WTs) and normal parotid parenchyma measured by using 12 concentric round ROIs and comparisons of the parameters among the three groups

ROI size (mm^2)	ADC				ADC_{SD}				Homogeneity index			
	PA (n=37)	WT (n=36)	Normal parotid parenchyma (n=56)	P#,*	PA (n=37)	WT (n=36)	Normal parotid parenchyma (n=56)	P#,§	PA (n=37)	WT (n=36)	Normal parotid parenchyma (n=56)	P#,*
9	1.72±0.39	1.17±0.46	0.94±0.24	<0.001	0.09±0.05	0.11±0.07	0.14±0.07	<0.001	0.05±0.03	0.10±0.06	0.16±0.09	<0.001
28	1.73±0.38	1.17±0.47	0.94±0.22	<0.001	0.12±0.07	0.15±0.09	0.19±0.08	<0.001	0.07±0.04	0.12±0.06	0.21±0.10	<0.001
34	1.73±0.38	1.17±0.47	0.94±0.21	<0.001	0.13±0.07	0.15±0.10	0.20±0.08	<0.001	0.08±0.04	0.13±0.07	0.22±0.11	<0.001
50	1.73±0.38	1.17±0.46	0.94±0.20	<0.001	0.15±0.07	0.17±0.11	0.21±0.08	<0.001	0.09±0.04	0.14±0.06	0.23±0.10	<0.001
60	1.73±0.38	1.17±0.46	0.94±0.19	<0.001	0.15±0.07	0.17±0.11	0.22±0.08	<0.001	0.09±0.04	0.14±0.07	0.24±0.11	<0.001
82	1.73±0.38	1.17±0.45	0.94±0.19	<0.001	0.17±0.07	0.19±0.13	0.23±0.08	<0.01	0.10±0.04	0.16±0.07	0.25±0.11	<0.001
93	1.73±0.38	1.16±0.45	0.94±0.19	<0.001	0.18±0.07	0.19±0.13	0.23±0.09	<0.01	0.11±0.04	0.16±0.07	0.25±0.10	<0.001
98	1.73±0.38	1.16±0.44	0.95±0.19	<0.001	0.18±0.07	0.20±0.13	0.23±0.08	<0.01	0.11±0.05	0.16±0.07	0.25±0.10	<0.001
115	1.72±0.38	1.16±0.43	0.95±0.18	<0.001	0.19±0.08	0.21±0.13	0.24±0.09	<0.01	0.12±0.05	0.17±0.08	0.26±0.10	<0.001
130	1.72±0.38	1.16±0.43	0.94±0.18	<0.001	0.20±0.08	0.21±0.14	0.24±0.08	<0.01	0.12±0.06	0.18±0.08	0.26±0.10	<0.001
136	1.72±0.37	1.16±0.42	0.94±0.18	<0.001	0.20±0.08	0.22±0.14	0.24±0.18	<0.01	0.12±0.06	0.18±0.08	0.26±0.10	<0.001
149	1.71±0.37	1.15±0.42	0.94±0.18	<0.001	0.21±0.09	0.23±0.14	0.25±0.18	0.019	0.13±0.06	0.19±0.08	0.27±0.10	<0.001

*, Post-hoc analyses show significant differences of ADCs between any two groups (all P<0.017); §, no significant differences in mean ADC_{SD}s with each ROI between PA and WT (all P>0.017); #, Kruskal-Wallis tests. ADC, apparent diffusion coefficient; SD, standard deviation; ROI, region of interest.

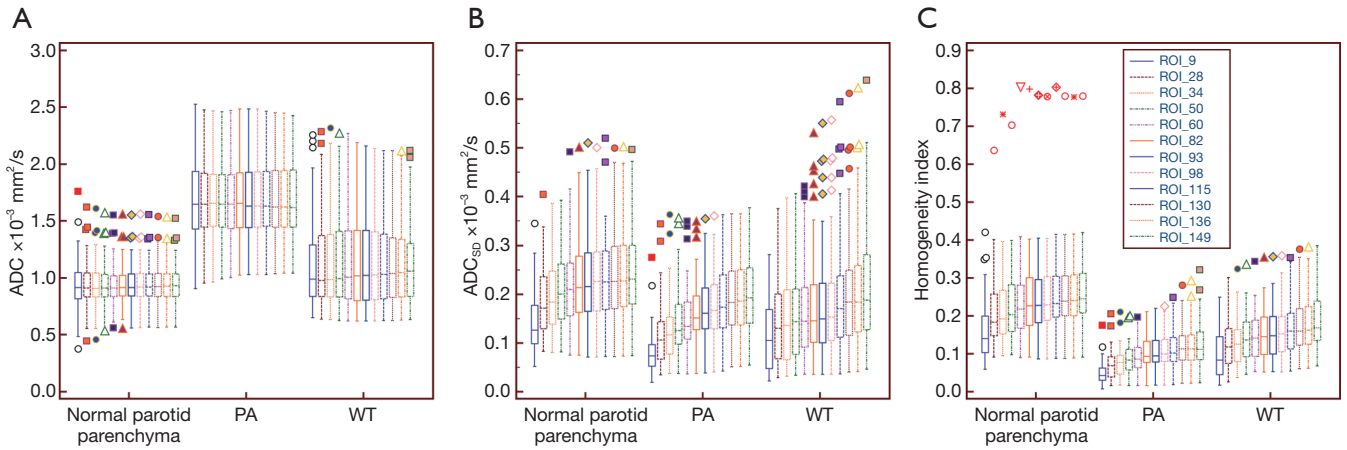

Figure 2 Box plots of the 12 regions of interest derived the mean apparent diffusion coefficient (ADC) (A), standard deviation (SD) of the ADC (ADC_{SD}) (B), and homogeneity index (C) for normal parotid parenchyma, pleomorphic adenomas (PA), and Warthin tumors (WT). The midline within each box represents the median value. Horizontal lines within boxes represent median values, vertical lines and whiskers denote 95% CIs. ROI, region of interest; CI, confidence interval.

Table 3 Diagnostic performances of the mean homogeneity indices obtained from the 12 ROIs for discriminating pleomorphic adenomas from normal parotid parenchyma

ROI size (mm^2)	Optimal cutoff values	AUC ± SE (95% CI)	Sensitivities (95% CI)	Specificities (95% CI)	PPV (%)	NPV (%)	ACC (%)
9	0.07	0.944±0.024 (0.876–0.981)	83.8 (68.0–93.8)	92.9 (82.7–98.0)	88.6	89.7	89.3
28	W0.11	0.955±0.022 (0.891–0.987)	89.2 (74.6–97.0)	91.1 (80.4–97.0)	86.9	92.7	90.3
34	0.11	0.954±0.022 (0.890–0.987)	83.8 (68.0–93.8)	96.4 (87.7–99.6)	93.9	90.0	91.4
50	0.13	0.954±0.021 (0.890–0.987)	91.9 (78.1–98.3)	91.1 (80.4–97.0)	87.2	94.5	91.4
60	0.14	0.952±0.020 (0.887–0.986)	91.9 (78.1–98.3)	91.1 (80.4–97.0)	87.2	94.5	91.4
82	0.16	0.949±0.021 (0.882–0.984)	91.9 (78.1–98.3)	87.5 (75.9–94.8)	82.9	94.2	89.3
93	0.17	0.945±0.022 (0.878–0.982)	91.9 (78.1–98.3)	85.7 (73.8–93.6)	80.9	94.1	88.2
98	0.16	0.943±0.023 (0.874–0.980)	89.2 (74.6–97.0)	87.5 (75.9–94.8)	82.5	92.5	88.2
115	0.17	0.930±0.027 (0.857–0.972)	89.2 (74.6–97.0)	87.5 (75.9–94.8)	82.5	92.5	88.2
130	0.16	0.925±0.029 (0.852–0.970)	83.8 (68.0–93.8)	94.6 (85.1–98.9)	91.1	89.8	90.3
136	0.16	0.922±0.031 (0.847–0.967)	83.8 (68.0–93.8)	94.6 (85.1–98.9)	91.1	89.8	90.3
149	0.16	0.915±0.034 (0.839–0.963)	83.8 (68.0–93.8)	94.6 (85.1–98.9)	91.1	89.8	90.3

ROC, receiver operating characteristic curve; AUC, area under curve; ADC, apparent diffusion coefficient; SE, standard error; CI, confidence interval; ROI, region of interest; PPV, positive predictive value; NPV, negative predictive value; ACC, accuracy.

for PA, WT, or normal parotid parenchyma. Thus, in the clinical practice, we recommend that ROI should be as large as possible according to the tumor sizes of PA and WT to reduce possible measurement errors.

Wang *et al.* reported that ADC_{SD} was an independent predictor of WT in differentiating between PA and carcinomas (26). However, in the current study, no significant differences were observed in the mean ADC_{SD} values of the 12 ROIs between PA and WT, which was inconsistent with the reports of Wang *et al.* The main reason for the different findings may be that the sources of patients in the two studies were different, and ROI methods

Table 4 Diagnostic performances of the mean homogeneity indices obtained from 12 ROIs for discriminating Warthin tumor from normal parotid parenchyma

ROI size (mm^2)	Optimal cutoff values	AUC ± SE (95% CI)	Sensitivities (95% CI)	Specificities (95% CI)	PPV (%)	NPV (%)	ACC (%)
9	0.09	0.723±0.056 (0.620–0.811)	55.6 (38.1–72.1)	82.1 (69.6–91.1)	66.6	74.2	71.7
28	0.15	0.784±0.049 (0.686–0.863)	66.7 (49.0–81.4)	78.6 (65.6–88.4)	66.7	78.6	73.9
34	0.17	0.793±0.048 (0.696–0.870)	80.1 (64.0–91.8)	71.4 (57.8–82.7)	64.3	84.8	74.8
50	0.19	0.793±0.047 (0.696–0.871)	86.1 (70.5–95.3)	60.7 (46.8–73.5)	58.5	87.2	70.6
60	0.17	0.790±0.048 (0.693–0.868)	72.2 (54.8–85.8)	73.2 (59.7–84.2)	63.4	80.4	72.8
82	0.18	0.776±0.051 (0.677–0.857)	75.0 (57.8–87.9)	73.2 (59.7–84.2)	64.3	82.0	73.9
93	0.19	0.777±0.051 (0.679–0.857)	72.2 (54.8–85.8)	75.0 (61.6–85.6)	65.0	80.8	73.9
98	0.19	0.779±0.052 (0.681–0.859)	75.0 (57.8–87.9)	75.0 (61.6–85.6)	65.9	82.4	75.0
115	0.19	0.774±0.053 (0.675–0.855)	72.2 (54.8–85.8)	78.6 (65.6–88.4)	68.4	81.5	76.1
130	0.18	0.773±0.054 (0.674–0.854)	61.1 (43.5–76.9)	87.5 (75.9–94.8)	75.9	77.8	77.2
136	0.20	0.765±0.055 (0.665–0.847)	66.7 (49.0–81.4)	83.4 (67.6–89.8)	72.1	79.6	76.9
149	0.17	0.752±0.057 (0.652–0.837)	55.6 (38.1–72.1)	94.6 (85.1–98.9)	86.9	76.8	79.3

ROC, receiver operating characteristic curve; AUC, area under curve; ADC, apparent diffusion coefficient; SE, standard error; CI, confidence interval; ROI, region of interest; PPV, positive predictive value; NPV, negative predictive value; ACC, accuracy.

Table 5 Diagnostic performances of the mean homogeneity indices obtained from the 12 ROIs for discriminating pleomorphic adenomas from Warthin tumor

ROI size (mm^2)	Optimal cutoff values	AUC ± SE (95% CI)	Sensitivities (95% CI)	Specificities (95% CI)	PPV (%)	NPV (%)	ACC (%)
9	0.07	0.731±0.061 (0.615–0.828)	63.9 (46.2–79.2)	83.8 (68.0–93.8)	79.3	70.5	74.0
28	0.10	0.742±0.059 (0.627–0.838)	63.9 (46.2–79.2)	83.8 (68.0–93.8)	79.3	70.5	74.0
34	0.11	0.746±0.059 (0.631–0.841)	63.9 (46.2–79.2)	83.8 (68.0–93.8)	79.3	70.5	74.0
50	0.12	0.740±0.059 (0.624–0.836)	61.1 (43.5–76.9)	91.1 (68.0–93.8)	87.0	70.6	76.3
60	0.12	0.735±0.059 (0.619–0.831)	61.1 (43.5–76.9)	81.1 (64.8–92.0)	75.9	68.2	71.2
82	0.14	0.734±0.059 (0.618–0.831)	61.1 (43.5–76.9)	81.1 (64.8–92.0)	75.9	68.2	71.2
93	0.14	0.730±0.059 (0.614–0.828)	55.6 (38.1–72.1)	83.8 (68.0–93.8)	77.0	66.0	69.9
98	0.14	0.734±0.059 (0.618–0.831)	61.1 (43.5–76.9)	78.4 (61.8–90.2)	73.3	67.4	69.9
115	0.17	0.738±0.058 (0.622–0.834)	50.0 (32.9–67.1)	89.2 (74.6–97.0)	81.8	64.7	69.9
130	0.12	0.734±0.059 (0.618–0.831)	80.1 (64.0–91.8)	56.8 (39.5–72.9)	64.3	74.6	68.3
136	0.12	0.742±0.058 (0.627–0.838)	77.8 (60.8–89.9)	62.2 (44.8–77.5)	66.7	74.2	69.9
149	0.12	0.749±0.058 (0.634–0.843)	86.1 (70.5–95.3)	59.5 (42.1–75.2	67.4	81.5	72.6

ROC, receiver operating characteristic curve; AUC, area under curve; ADC, apparent diffusion coefficient; SE, standard error; CI, confidence interval; ROI, region of interest; PPV, positive predictive value; NPV, negative predictive value; ACC, accuracy.

used in the two studies for ADC and SD measurements were different. It was worth mentioning that homogeneity index may be a useful parameter in differentiating between PA, WT, and normal parotid parenchyma. The higher the index was, the more heterogeneous the ADC in the area was. In particular, the homogeneity index had higher accuracies in helping differential diagnosis of PA and WT than with ADCs.

Some ROI methods including the whole-volume ROI, selected-slice ROI, and small-sample ROI approaches have been applied in tumor ADC measurements (22). For the whole-volume method, ROIs cover the entire tumor area on each tumor-containing slice. For the single-slice method, ROIs cover the whole tumor on the largest observed tumor area slice. For the small-sample method, a round/oval ROI is placed on the solid portion of the tumor. The effects of ROI methods on ADC measurements have been investigated in some tumors, and each ROI method has its own advantages and disadvantages (27-29). Whole-volume ROI can reduce inter- or intra-observer variability in ADC measurements; however, it is time-consuming and its application is limited in clinical practice (21,22). Ma *et al.* reported that ADCs obtained from small-sample ROIs could provide greater diagnostic performance than the selected-slice or whole-volume ROI methods in the assessment of pancreatic cancer (21). The small-sample ROI method is the most commonly used in practice. In addition, it is difficult to delineate ROI when using the whole-volume or selected-slice ROI methods in WT with secondary infection because of the untidy margin of tumors (30,31). This being the case, the small-sample ROI approach was used and assessed in the current study.

This study had some limitations. First, it was carried out retrospectively, which made it difficult to control all aspects of this study. Second, the patient population was relatively small, and a larger sample size is needed to confirm the results in the future. In addition, the effects of ROI sizes on ADC measurements of malignant tumors of the parotid gland were not investigated because of the limited cases of malignant tumors of parotid gland in the data collection of this study. Third, DWI was only performed with two b-values (0 and 1,000 s/mm^2) in the study; the choice of b-values may cause the large range of ADCs, because it has been shown that the lower the b-values, the higher the contribution of perfusion, and the use of higher b values may be more sensitive to reflect true diffusion (32). Ideally, multi-b-value DWI should be used for more accurate measurement of ADC (33). Fourth, we did not compare the ADCs from different ROI approaches. This might have led to bias in the results because different slices might be able to have provided various ADCs. Finally, the influence of image distortion on ADCs for parotid masses was not analyzed. Imaging distortion and signal loss having potential influences on ADCs of normal parotid parenchyma on echo-planar DWI have been reported (34,35), and this influence might have affected our results.

Our results revealed that ROI size had no significant influence on the differentiation among PA, WT, and normal parotid parenchyma. Homogeneity index was a useful parameter in differentiating between the three groups. This study suggested that the effect of ROI size on ADC measurements could be excluded from the differentiation of PA, WT, and normal parotid parenchyma.

Acknowledgements

None.

Footnote

Conflicts of Interest: The authors have no conflicts of interest to declare.

Ethical Statement: Institutional review board approval of Shanghai Ninth People's Hospital Ethics Committee was obtained for this study.

References

1. Przewoźny T, Stankiewicz C. Neoplasms of the parotid gland in northern Poland, 1991-2000: an epidemiologic study. Eur Arch Otorhinolaryngol 2004;261:369-75.
2. Wang J, Takashima S, Takayama F, Kawakami S, Saito A, Matsushita T, Momose M, Ishiyama T. Head and neck lesions: characterization with diffusion-weighted echo-planar MR imaging. Radiology 2001;220:621-30.
3. Matsusue E, Fujihara Y, Matsuda E, Tokuyasu Y, Nakamoto S, Nakamura K, Ogawa T. Differentiating parotid tumors by quantitative signal intensity evaluation on MR imaging. Clin Imaging 2017;46:37-43.
4. Yerli H, Aydin E, Haberal N, Harman A, Kaskati T, Alibek S. Diagnosing common parotid tumours with magnetic resonance imaging including diffusion-weighted imaging vs fine-needle aspiration cytology: a comparative study. Dentomaxillofac Radiol 2010;39:349-55.
5. Habermann CR, Arndt C, Graessner J, Diestel L, Petersen

KU, Reitmeier F, Ussmueller JO, Adam G, Jaehne M. Diffusion-weighted echo-planar MR imaging of primary parotid gland tumors: is a prediction of different histologic subtypes possible? AJNR Am J Neuroradiol 2009;30:591-6.
6. Yologlu Z, Aydin H, Alp NA, Aribas BK, Kizilgoz V, Arda K. Diffusion weighted magnetic resonance imaging in the diagnosis of parotid masses. Preliminary results. Saudi Med J 2016;37:1412-6.
7. Antony J, Gopalan V, Smith RA, Lam AK. Carcinoma ex pleomorphic adenoma: a comprehensive review of clinical, pathological and molecular data. Head Neck Pathol 2012;6:1-9.
8. Hisatomi M, Asaumi J, Yanagi Y, Unetsubo T, Maki Y, Murakami J, Matsuzaki H, Honda Y, Konouchi H. Diagnostic value of dynamic contrast-enhanced MRI in the salivary gland tumors. Oral Oncol 2007;43:940-7.
9. Motoori K, Ueda T, Uchida Y, Chazono H, Suzuki H, Ito H. Identification of Warthin tumor: magnetic resonance imaging versus salivary scintigraphy with technetium-99m pertechnetate. J Comput Assist Tomogr 2005;29:506-12.
10. Yerli H, Agildere AM, Aydin E, Geyik E, Haberal N, Kaskati T, Oguz D, Ozluoglu LN. Value of apparent diffusion coefficient calculation in the differential diagnosis of parotid gland tumors. Acta Radiol 2007;48:980-7.
11. Supsupin EP Jr, Demian NM. Magnetic resonance imaging (MRI) in the diagnosis of head and neck disease. Oral Maxillofac Surg Clin North Am 2014;26:253-69.
12. Hamilton BE, Salzman KL, Wiggins RH 3rd, Harnsberger HR. Earring lesions of the parotid tail. AJNR Am J Neuroradiol 2003;24:1757-64.
13. Ikeda K, Katoh T, Ha-Kawa SK, Iwai H, Yamashita T, Tanaka Y. The usefulness of MR in establishing the diagnosis of parotid pleomorphic adenoma. AJNR Am J Neuroradiol 1996;17:555-9.
14. Vogl TJ, Dresel SH, Späth M, Grevers G, Wilimzig C, Schedel HK, Lissner J. Parotid gland: plain and gadolinium-enhanced MR imaging. Radiology 1990;177:667-74.
15. Mikaszewski B, Markiet K, Smugała A, Stodulski D, Szurowska E, Stankiewicz C. Diffusion-weighted MRI in the differential diagnosis of parotid malignancies and pleomorphic adenomas: can the accuracy of dynamic MRI be enhanced? Oral Surg Oral Med Oral Pathol Oral Radiol 2017;124:95-103.
16. Srinivasan A, Dvorak R, Perni K, Rohrer S, Mukherji SK. Differentiation of benign and malignant pathology in the head and neck using 3T apparent diffusion coefficient values: early experience. AJNR Am J Neuroradiol 2008;29:40-4.
17. Sumi M, Van Cauteren M, Sumi T, Obara M, Ichikawa Y, Nakamura T. Salivary gland tumors: use of intravoxel incoherent motion MR imaging for assessment of diffusion and perfusion for the differentiation of benign from malignant tumors. Radiology 2012;263:770-7.
18. Ma G, Zhu LN, Su GY, Hu H, Qian W, Bu SS, Xu XQ, Wu FY. Histogram analysis of apparent diffusion coefficient maps for differentiating malignant from benign parotid gland tumors. Eur Arch Otorhinolaryngol 2018;275:2151-7.
19. Eida S, Sumi M, Sakihama N, Takahashi H, Nakamura T. Apparent diffusion coefficient mapping of salivary gland tumors: prediction of the benignancy and malignancy. AJNR Am J Neuroradiol 2007;28:116-21.
20. Fruehwald-Pallamar J, Czerny C, Holzer-Fruehwald L, Nemec SF, Mueller-Mang C, Weber M, Mayerhoefer ME. Texture-based and diffusion-weighted discrimination of parotid gland lesions on MR images at 3.0 Tesla. NMR Biomed 2013;26:1372-9.
21. Ma C, Liu L, Li J, Wang L, Chen LG, Zhang Y, Chen SY, Lu JP. Apparent diffusion coefficient (ADC) measurements in pancreatic adenocarcinoma: A preliminary study of the effect of region of interest on ADC values and interobserver variability. J Magn Reson Imaging 2016;43:407-13.
22. Lambregts DM, Beets GL, Maas M, Curvo-Semedo L, Kessels AG, Thywissen T, Beets-Tan RG. Tumour ADC measurements in rectal cancer: effect of ROI methods on ADC values and interobserver variability. Eur Radiol 2011;21:2567-74.
23. Ma C, Guo X, Liu L, Zhan Q, Li J, Zhu C, Wang L, Zhang J, Fang X, Qu J, Chen S, Shao C, Lu JP. Effect of region of interest size on ADC measurements in pancreatic adenocarcinoma. Cancer Imaging 2017;17:13.
24. Attyé A, Troprès I, Rouchy RC, Righini C, Espinoza S, Kastler A, Krainik A. Diffusion MRI: literature review in salivary gland tumors. Oral Dis 2017;23:572-5.
25. Thoeny HC, De Keyzer F, King AD. Diffusion-weighted MR imaging in the head and neck. Radiology 2012;263:19-32.
26. Wang CW, Chu YH, Chiu DY, Shin N, Hsu HH, Lee JC, Juan CJ. JOURNAL CLUB: The Warthin Tumor Score: A Simple and Reliable Method to Distinguish Warthin Tumors From Pleomorphic Adenomas and Carcinomas. AJR Am J Roentgenol 2018;210:1330-7.
27. Tsili AC, Ntorkou A, Astrakas L, Xydis V, Tsampalas S, Sofikitis N, Argyropoulou MI. Diffusion-weighted

magnetic resonance imaging in the characterization of testicular germ cell neoplasms: Effect of ROI methods on apparent diffusion coefficient values and interobserver variability. Eur J Radiol 2017;89:1-6.
28. Mahmood F, Johannesen HH, Geertsen P1, Opheim GF, Hansen RH. The effect of region of interest strategies on apparent diffusion coefficient assessment in patients treated with palliative radiation therapy to brain metastases. Acta Oncol 2015;54:1529-34.
29. Mukuda N, Fujii S, Inoue C, Fukunaga T, Tanabe Y, Itamochi H, Ogawa T. Apparent diffusion coefficient (ADC) measurement in ovarian tumor: Effect of region-of-interest methods on ADC values and diagnostic ability. J Magn Reson Imaging 2016;43:720-5.
30. Habermann CR, Gossrau P, Graessner J, Arndt C, Cramer MC, Reitmeier F, Jaehne M, Adam G. Diffusion-weighted echo-planar MRI: a valuable tool for differentiating primary parotid gland tumors? Rofo 2005;177:940-5.
31. Matsushima N, Maeda M, Takamura M, Takeda K. Apparent diffusion coefficients of benign and malignant salivary gland tumors. Comparison to histopathological findings. J Neuroradiol 2007;34:183-9.
32. Thoeny HC, De Keyzer F, Boesch C, Hermans R. Diffusion-weighted imaging of the parotid gland: Influence of the choice of b-values on the apparent diffusion coefficient value. J Magn Reson Imaging 2004;20:786-90.
33. Padhani AR, Liu G, Koh DM, Chenevert TL, Thoeny HC, Takahara T, Dzik-Jurasz A, Ross BD, Van Cauteren M, Collins D, Hammoud DA, Rustin GJ, Taouli B, Choyke PL. Diffusion-weighted magnetic resonance imaging as a cancer biomarker: consensus and recommendations. Neoplasia 2009;11:102-5.
34. Juan CJ, Chang HC, Hsueh CJ, Liu HS, Huang YC, Chung HW, Chen CY, Kao HW, Huang GS. Salivary glands: echo-planar versus PROPELLER Diffusion-weighted MR imaging for assessment of ADCs. Radiology 2009;253:144-52.
35. Liu YJ, Lee YH, Chang HC, Huang TY, Chiu HC, Wang CW, Chiou TW, Hsu K, Juan CJ, Huang GS, Hsu HH. A potential risk of overestimating apparent diffusion coefficient in parotid glands. PLoS One 2015;10:e0124118.

Cite this article as: Sun Q, Ma C, Dong M, Jiang M, Tao X. Effects of region of interest sizes on apparent diffusion coefficient measurements of pleomorphic adenoma, Warthin tumor, and normal parotid parenchyma. Quant Imaging Med Surg 2019;9(4):681-690. doi: 10.21037/qims.2019.04.11

